Statistical Tolerance and Clearance Analysis for Assembly

Sukhan Lee[1,2] and Chunsik Yi[1]

Department of Computer Science[1]
University of Southern California
Los Angeles, CA 90089-0781

Jet Propulsion Laboratory[2]
California Institute of Technology
Pasadena, CA 91109

Abstract

Tolerance is inevitable because manufacturing exactly equal parts is known to be impossible. Furthermore, the specification of tolerances is an integral part of product design since tolerances directly affect the assemblability, functionality, manufacturability, and cost effectiveness of a product. In this paper, we present statistical tolerance and clearance analysis for the assembly. Tolerances work against the assemblability of a product since they can propagate and accumulate in the product, making it more difficult or impossible to assemble. Clearances, however, work for the assemblability since they can be used to compensate for tolerances. The poses of parts in an assembly may be adjusted within the permitted clearances to assemble the parts. Monte-Carlo method is used in the analysis, with Gaussian distribution, Gaussian-Sigmoid distribution, and Chi-Square error reduction scheme to approximate tolerances and clearances. Then, algorithms to compute the propagation of tolerances and clearances are proposed. Our proposed work is expected to make the following contributions: (i) to help the designers to evaluate products for assemblability, (ii) to provide a new perspective to tolerance problems, and (iii) to provide a tolerance analysis tool which can be incorporated into a CAD or solid modeling system.

1: Introduction

The specification of tolerances is an integral part of a product design since tolerances directly affect the assemblability, functionality, and manufacturability of a product. Moreover, tolerance is inevitable because manufacturing exactly equal parts is known to be impossible [1].

Although they are small as compared with part dimensions, tolerances can propagate and accumulate in an assembly affecting the product assemblability. For example, an assembly with six nominal parts is shown in Fig. 1 (a). It may fail to assemble if some manufactured parts deviate from their nominal shape. Fig. 1 (b) shows that two pegs of P1 deviate from their nominal pose: one has a small rotation deviation and the other one has a small translation deviation. The assembly fails to assemble because these deviations propagate in the assembly, and make Some parts to intersect, e.g., P2 intersects with P4 and P6, and P4 intersects with P5 and P6.

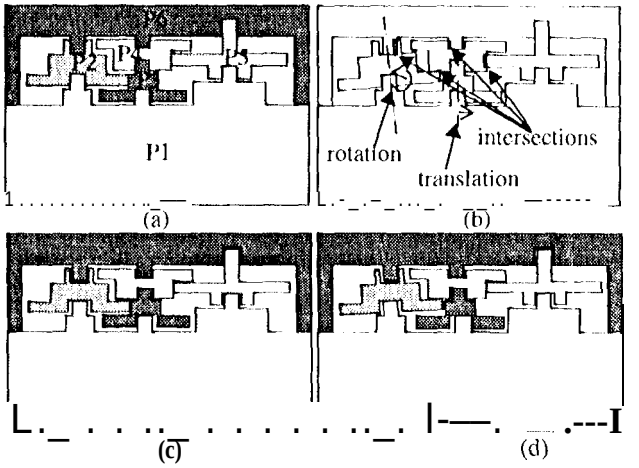

Figure 1: An assembly with six parts.

Clearances can be used to compensate for tolerances. Clearance is a free, adjustable space between two mating features, which are surfaces of parts that play a functional role in an assembly. This free may be used for adjusting the part poses. For example, Fig. 1 (c) shows that an assembly is designed with clearances. This assembly may be assembled with toleranced P1 because the clearances can be used to adjust the poses of parts in the assembly to compensate the deviations caused by the tolerances, as shown in Fig. 1 (d). Note that P1 in Fig. 1 (b) is just one feasible instance of shape deviations of P1. For example, a peg feature of P1 is allowed to have any deviation within the tolerance specification, as shown in Fig. 2. Fig. 2(a) shows that the feature has position tolerance. The meaning of the position tolerance is that the axis of the feature is allowed to be anywhere within the tolerance zone, as shown in Fig. 2(b). (Refer to [2,3] for more details of tolerance specifications.)

The goal of this work is to study the effect of tolerances and clearances on the assemblability of a product. That is, what is the assemblability, or the probability of successful assembly, of a product under the given tolerances and clearances? The assemblability of a product is an important issue in design because it is directly related to the cost and productivity.

In this work, tolerance is represented by an ellipsoid, with Gaussian distribution, and clearance is represented by a nominal ellipsoid and a range. The nominal ellipsoid represents an approximation of nominal clearance.

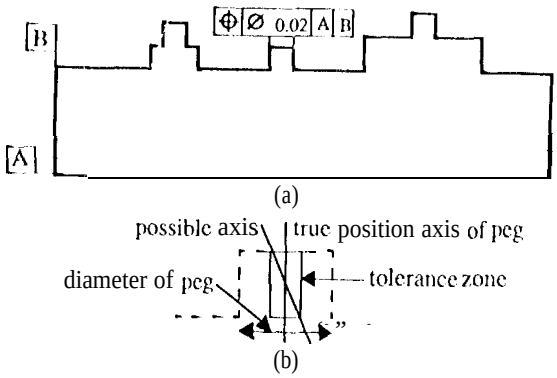

Figure 2: Position tolerance of a peg in 2-D.

Whereas the range represents the permitted statistical variability of the nominal clearance. Monte-carlo method is used to simulate the. tolerances of mating features. q'hen, Gaussian distribution and Chi-Square error reduction scheme are used to approximate. the tolerances; and Gaussian-Sigmoid distribution and (lhi-Square error reduction scheme are used to approximate the clearances. For the analysis, following assumptions arc made: Parts arc assumed to be rigid and do not de form during assembly; clearance between mating features are zero or larger; exactly two mating features arc used in mating; and the assembly is assumed to have no intersection between nominal parts in an assembly.

2: Related works

Whitney and Gilbert [4] represented tolerance by a transform matrix in kinematic parameters to be used as input to a tolerance analysis tool. By using the Chi-Squ are error reduction scheme, they minimized the probability error between the analytic solution of a Gaussian probability density function and the simulated solution from Monte-Carlo simulation. A possible representation for clearance between two mating features was proposed briefly in terms o f conditional variance. However, neither the representation nor tbc computation for clearance was provided. In particular, clearance was described in the context of tolerance propagation treating it as tolerance (uncertainty.) Foster [2] anti ANSI Y14.5M[3] describe geometric dimensioning anti tolerancing for designing ami manufacturing components of a mechanical products. Requicha [5,6] proposed a tolerance zone representation in an effort to integrate it with solid modelers. This representation uses tolerance zones to check whether the appropriate portions of the part boundary lie within the zones.

Bjorke [1] proposed one dimensio nal statistical tolerancc analysis based on the function ality of a product. His objective was to derive the tolerance chain equation for a sum dimension, an important dimension in a product. Then, the sum dimension was checked whether or not it met the functionality criteria, e.g., a clearance between two surfaces must be larger than zero and less than some limit. Treacy and et al. [7], Wang anti Ozsoy [8], and Soderberg [9] implemented a data structure, an algorithm

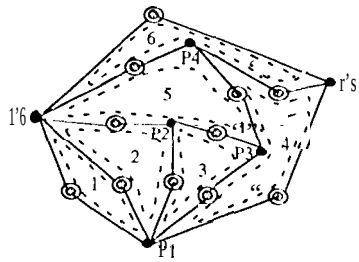

Figure 3: Feature graph of six part assembly.

for generating the tolerance chain, and a computer interfacc of Bjorke's approach.

Su and Lee [10] modeled tolerances using differential transforms and characterized them using means and covariances. They proposed an analytical method for tolerance propagations. However, the method did not consider clearance, and the approach was based on the pose uncertainty of an object during an assembly task. Shalon anti et ai. [11] computed the. expected worst-case location of a feature in an assembly using transformation matrix multiplications. Grossman [12] used Monte Carlo method to simulate manufacturing processes, where four holes arc drilled into a rectangular box. ~'hen, an assembly process was simulated where a lid with four holes was attached to a box with four holes, so that the four screws could be inserted. The number of successful assemblies was determined based on whether all screw holes were aligned within predefined limits.

3: Representation

This section describes in detail tolerance and clearance representations and computations involved in approximating the tolerances and clearances. An assembly model is also described briefly.

3.1: Assembly modeling by a feature graph

An assembly is modeled by a feature graph (FG.) FG describes both the local relations between a part and its mating features, and the global mating relations between tile parts in an assembly. In an assembly, parts are mated through mating features. A mating feature is a feature (or surface) of a part that plays a functional role such as mating, FG is similar to mating graph [13], but FG includes tolerance anti clearance attributes.

FG is defined by a set of nodes arid a set of edges: FG= (N,E). There are three types of nodes: F-node, M-node, anti P-node. F-node represents a mating feature, anti has an associated tolerance ellipsoid. M-node represents a pair of mating features, and has an associated clearance ellipsoid. Note that two 1~-nodes represent onc M-node. P-node represents a local coordinate frame of a part (e.g., datum reference frame.) An edge represents the relation between P-node and I;-node, and has the associated transformation matrix. In the pictures, F-node is denoted by a white or gray circle, M-node is denoted by a gray circle inside a white circle, and]'-node is denoted by a black cir-

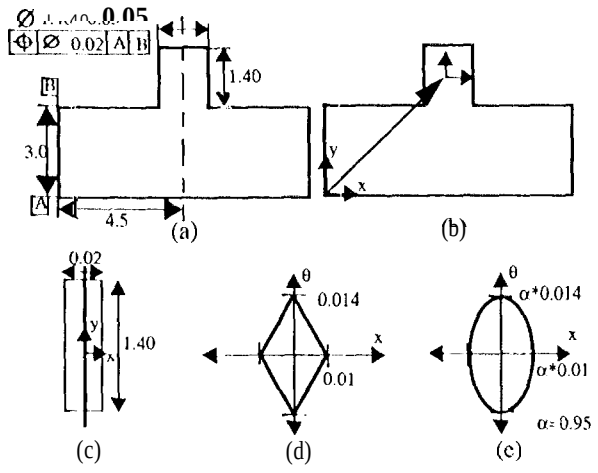

Figure 4: Pose tolerance and tolerance ellipsoid.

cle. For example, FG of six part assembly in Fig. 1 is shown in Fig. 3.

3.2: Tolerance representation

ANSI Y14.5M[2,3] defines various types of geometric tolerances, e.g., form, location, orientation, profile, and runout, to represent tolerance of a feature. 'There are two types of features: related and individual. Tolerances of most related features can be represented by ellipsoids [4]. Related features are features which relate to a datum, or datums, in location, orientation, runout, and profile. The tolerance of a related mating feature affects the pose of the feature, and is called pose *tolerance*. Where as, individual features are features which relate to perfect geometric counterparts of themselves as the desired forms, and no datum is used. The tolerance of an individual mating feature affects clearance, and is called *dimension tolerance.*

The *pose* tolerance (or tolerance) of a feature is represented by an ellipsoid with its center located at the origin of the nominal coordinate frame of the feature. Although there exist other types of distributions for manufacturing processes, e.g, rectangular, beta, etc., Gaussian distribution is assumed for pose and dimension tolerances because the specific manufacturing processes are not known at a design stage, many manufacturing processes have Gaussian distribution [9], and central limit theorem[9,14] can be applied to tolerance propagation.

The ellipsoid is an approximation of real tolerance described in kinematic parameters. For example, the peg feature shown in Fig. 4(a) has position tolerance of 0.02 in diameter. The meaning of the position tolerance [2,3] is that the axis of the peg is allowed to reside. in the tolerance zone defined by a rectangular box as shown in Fig. 4(c), This implies that the coordinate frame attached to the axis of the peg, as shown in Fig. 4(b), can translate maximum of ±0.01 in x-axis and rotate maximum of ±0.014 about z-axis (the axis orthogonal to the paper), as strewn in Fig. 4(d). This area is called tolerance volume, and shows that x and θ parameters are dependent. Finally, this tolerance volume is represented by an ellipse that optimally approximates the distribution of the tolerance volume, as shown in Fig. 4(e). The optimization factor, α= 0.95, is obtained from a simulation result using 5000 randomly and normally generated samples using the process described below. The simulated solution and the analytic solution are shown in Figs. 5(a) and (b), respectively.

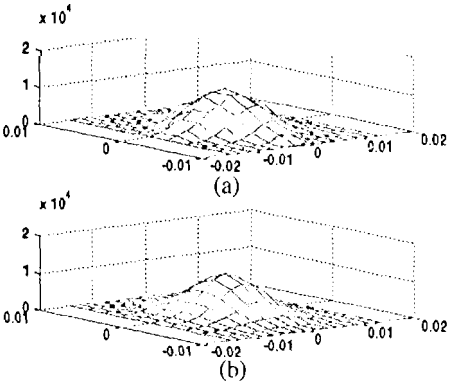

Figure 5: Simulated and analytic solutions,

The computation process of a tolerance ellipsoid is as follows: We assume that the tolerance has Gaussian distribution, and simulate the tolerance using Monte-carlo Method [1 S]. First, randomly and normally generate a point (x_i) On the x-axis within the maximum boundary (f O.O]). 'Then, randomly and normally generate a point (O_i) on the θ-axis within the limit at xi. The random sample (x_i,θ_i) is considered as an instance of one Monte-Carlo simulation. Repeat the random gene.[atic]~lNtiI[]cs. This is a simulated distribution of the. pose tolerance. Gaussian density function with σ, where σ is the standard deviation and equals to one-third of maximum boundary limits, is used to initially approximate the simulated density (e.g., σ_x= 0.01/3.) The probability within the ±3σ boundary of 2-D Gaussian distribution is 0.989[16]. This initial σ is optimized using Chi-Square error reduction scheme. In this scheme, the simulated area (total density is equal to one) and Gaussian density area (using ±3σ limits) are partitioned into square grids. "Then, for all grids, sum the squares of the. difference between two probabilities of the grid centers. Oli-Square. error reduction scheme iteratively multiplies σ's by an optimization factor, α, until the minimum Chi-Square is found for some α. The optimized ellipsoid has the axis lengths of α*3σ.

3.3: Clearance representation

Clearance a free, adjustable space between two mating features. This space provides adjustability to part poses in an assembly. When nominal dimensions of mating features are used, the corresponding clearance is nominal. However, dimension tolerances of mating features can create variability to the nominal clearance. The clearance between two mating features is represented by a nominal ellipsoid and a range with Gaussian distribution. Note that a functionality requirement may be associated with clear-

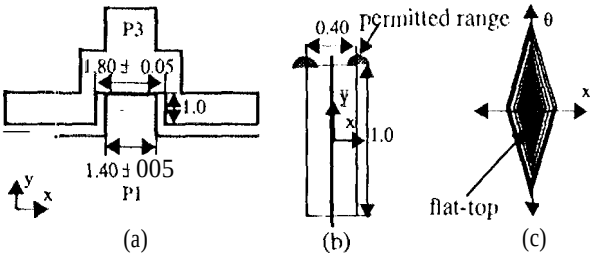

Figure 6: Clearance between peg and hole.

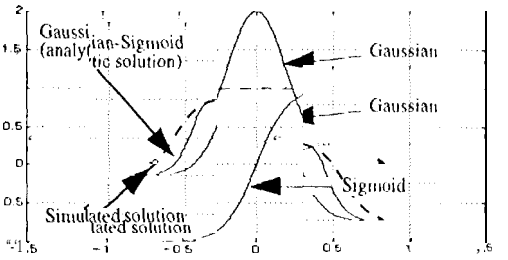

Figure 7: Clearance distributions.

ances. Therefore, clearance must accommodate functionality requirement.

A free space between two mating features is represented by a clearance zone. For example, the clearance zone of the peg and hole mating features of P1 and P3 in Fig. 6(a) is shown in Fig. 6(b). The axis of the clearance zone denotes the same axis of the peg. The nominal clearance zone is 0.4 by 1.0, which is the difference between the nominal diameters of the hole and peg, and the depth of the hole. Since the diameters of hole and peg have dimension tolerances of ±0.05, the clearance zone in x-axis have ±0.1 of variability. This range is assumed to have Gaussian distribution, as shown in Fig. 6(b). From this clearance zone and the range, clearance volumes can be generated, as shown in Fig. 6(c). This distribution is used for computing the. nominal clearance ellipsoid and the range.

The following algorithm Computes the clearance ellipsoid and the range of peg and hole mating features:

Algorithm: Clearance Ellipsoid (Peg-Hole)

1. Randomly and normally generate diameters, D_p, and D_h, Of the peg and hole., respectively. D_p is generated by adding the nominal peg diameter and the randomly and normally generated value, T_p, from the peg's dimension tolerance. T_p is generated using σ_p as the standard deviations of peg, where $\pm 3*\sigma_p$ is equal to the peg's dimension tolerance. D_h can be generated in a similar way. "I'he clearance zone is a rectangular area with the width, W, equals to $D_h - D_p$, and the height, H, equals to the depth of the hole.
2. Calculate the clearance volume from the clearance zone. When the axis orientation is zero, the limit in x-axis is equal to ± W/2. When the transla tion of the axis is zero, the. limit in rotation, O, is W/l J using the small angle approximation. The clearance volume has a diamond shape, which shows the dependency between x and O parameters.
3. Generate N clearance volumes from steps 1 and 2.
4. Generate M uniformly distributed samples, S_c, inside a square area which can cover the largest clearance volume.
5. For each clearance volume Vi, for i= 1,N, collect $S_i \subseteq S_c$ which intersect V_i. This collection Of S_i's form s a flat-top shape distribution. The flat-top area corresponds to the minimum clearance volume. (See Fig. 6(c).)
6. Using Gaussian-Sigmoid filter method, calculate the nominal clearance ellipsoid and its range. This step is discussed in next section in detail.

4: Clearance computation

This section shows the details of the computation process for calculating the nominal clearance ellipsoid and the range from a simulated solution of clearance.

4.1: Gaussian-Sigmoid filter

A simulated solution is approximated by an analytic solution, Gaussian-Sigmoid distribution. The simulated solution of clearance has a flat-top bell shape, as shown in Fig. 7 by a dotted line; and an analytic solution will approximate the shape, as shown in the figure. Sigmoid function is shown in equation (1).

$$S(Y) = 2\left[\frac{1}{1+e^{-Y/T}} - \frac{1}{2}\right] \qquad (1)$$

When, $Y = G(X)$, where $G(X)$ is a Gaussian probability density function (2),

$$G(X) = \frac{1}{(2\pi)^{n/2}|\Sigma|^{1/2}} e^{-\frac{1}{2}X^T\Sigma^{-1}X} \qquad (2)$$

the equation (1) becomes Gaussian-Sigmoid density function. This analytic solution has a shape similar to a clearance distribution. Two parameters, Σ and T, in Gaussian-Sigmoid function control the shape. Therefore, optimal values of these parameters should provide an optimal approximation of a simulated solution by an analytic solution.

The covariance matrix, Σ, of a simulated solution is computed using equation (3),

$$\Sigma = \frac{\sum_{i=1}^{M} \left(pt_i^T \times pt_i\right)}{A1} \qquad (3)$$

where M is the number of clearance samples and pt_i is the i_{th} sample. We. assume that the mean is at the origin of a coordinate frame. Note that Σ may not be a diagonal matrix, meaning that the matrix has rotational components. However, we can always compute the eigen values, A, and orthogonal eigen vectors, V, which con espond to the diagonal matrix and the rotation matrix of Σ, respec-

tively, or $\Sigma = V\Lambda V^{1}$ [1 7]. Note that throughout this paper, wc will assume that Σ is a diagonal matrix, unless stated otherwise.. This Σ is used as an initial covariance matrix in Gaussian-Sigmoid function (1).

The flat-top surface can be controlled by adjusting parameter '1' in Sigmoid-Gaussian function. '1' controls the. slope of the Sigmoid curve, which, in turn, controls the area of the flat-top surface of Gaussian-Sigmoid distribution. Optimal T provides an analytic fiat-top surface. that best fits an simulated flat-top surface. '1'hen, Σ is optimized to best fit the bell shape curve of a simulated solution.

4.2: optimization proms

Gradient-based method is used to optimize parameter T and to find the optimizing factor, c, for Σ, so that an analytic solution can best approximate a simulated solution. The Chi-Square (X^2) error equation used in this problem is the sum of the square errors between the analytic and simulated densities, as shown in equation (4).

$$\chi^2 = \sum_{i=}^{n} \sum_{1j=1}^{m} \left(S\left(X_{i,j}\right) - P\left(X_{i,j}\right)\right)^2 \qquad (4)$$

in this equation, $S(X_{ij})$ is the analytical density at $X_{i,j,}$ and $P(X_{i,j})$ is the simulated density at $X_{i,j}$, where $X_{i,j}$ is the grid(i,j). S and P arc. normalized such that the total density equals one.

The normalization may produce, some grid densities of a simulated solution larger than one. This is due to tbc random generation of samples. '1'0 take this case into account, the optimization of a flat-top sul.face begins oy adding the areas of the grids that have the density close to 1 (e. g., 0.95) or larger. This sum, A_{FT}, is an approxin nation of the area of a simulated flat-top sLu-face. From this, an initial T value can be computed for the Gaussian-Sigmoid functi on.

For an initial T value, the. minimum ellipsoid, E_{min}, is calculated from A_{FT} and the ratio, $\rho = \sigma_1^2/\sigma_2^2$. The ratio comes from the ratio of covariances of clearance samples. This E_{min} has the area equal to A_{FT}. The axis lengths of E_{min} are a and b of $A_{FT} = \pi ab$, where $a = \rho b$ and $b = \sqrt{A_{FT}/(\pi\rho)}$. Then, T can be computed with X=(a,0), or X=(0,b), as shown in equation (5).

$$T = \frac{-k}{\log\left[\left(2/(0.9985 - 1)\right) - 1\right]}, \text{ where} \qquad (5)$$

$$k = -\frac{1}{(2\pi)^{n/2}|\Sigma|^{1/2}} e^{-\frac{1}{2}X^T\Sigma^{-1}X}$$

However, this T gives an approximation of the area ofa simulated flat-top surface, and T can be optimized to better approximate the area with respect to the density of the flat-top area. That is, the density in the flat-top area of a simulated solution is not flat, Therefore, this actual density must be approximated by adjusting the '1'value.

Optimal '1' should have minimal error between the. densities of simulate.d and analytic solutions, only in the area of the flat-top surface of a simulated solution. Chi-Square crmr equation can be formulated such that the densities outside the flat-top area arc zero for both solutions. Gradient δT of T can be formulated as shown in equation (6).

$$\delta T = -\alpha\frac{\partial\chi^2}{\partial T} = -\alpha \sum_{i=1}^{n} \sum_{j=1}^{m} \left\{2\left(S\left(X_{i,j}\right) - P\left(X_{i,j}\right)\right)\frac{\partial S}{\partial T}\right\} \qquad (6)$$

At each iteration of the Chi-Square error reduction scheme, δT is added to T, until T converges (or X^2 reaches its predefined limit set by a user.) This T_{opt} is an optimal T for given Σ.

Next, Σ is optimized to best fit the density between tbc flat-top surface anti the. boundary of a simulated solution by an analytic solution. When optimizing Σ, T_{opt} must also change accordingly to preserve an optimal flat-top area. Gradient δc for the optimization factor c of Σ is computed. δc can be formulated as in equation **(7).**

$$\delta c = -\beta\frac{\partial\chi^2}{\partial c} = -\beta \sum_{i=1}^{n} \sum_{1j=1}^{m} \left\{2\left(S\left(X_{i,j}, c\Sigma\right) - P\left(X_{i,j}\right)\right)\frac{\partial S}{\partial c}\right\} \qquad (7)$$

During Chi-Square error reduction iterations, δc is added to c. 'J'hen, Σ is multiplied by c. The density inside the flat-top area is kept zero since optimization process is performed outside this area,

I inally, the. clearance ellipsoid and the range can be computed from the minimum and maximum ellipsoids derived from equation (1) by letting S(Y)= Z, where Z equal to 0.9985 and 0.0015, respectively. These Z value.s are selected as they closely correspond to $\pm 3\sigma$ probability y of Gaussian distribution [16]. The ellipsoid equation derived from equation (1) is shown in equation (8)

$$1 = \frac{1}{r}\mathbf{X}^T\mathbf{X}\mathbf{1}\mathbf{X}, \text{ where} \qquad (8)$$
$$, 2 \quad -2Ln\left[\left(-TLn\left(\frac{1-Z}{1+Z}\right)\right)\left((2\pi)^{n/2}|\Sigma|^{1/2}\right)\right]$$

The nominal clearance ellipsoid is the average ellipsoid of the two ellipsoids, i.e., axis lengths of the nominalellipsoid arc the aver-:igc lengths of the two ellipsoids. The range is the diffc.rent.c between the axis lengths of the nominal anti the minimum ellipsoid (or maximum ellipsoid.)

The following example shows the computation process and results of a simulation for the clearance ellipsoid and the range between two mating features, peg and hole, of P1 anti P3 shown in Fig. 6(a). Wc performed Monte-Carlo simulation on the diameter dimensions of the peg and the hoic with N= 50. This results in 50 possible clearance zones and volu mes. S= 2500 random and uni form samples were gencrated within the maximum boundary, Then, all samples $S_i \subseteq S$ that intersect with clearance volumes are collected, for all N clearance volumes. The corresponding nor malized density mesh of the simulated clearance is shown in Fig. 8(a). The clearance area was partitioned into square grids with longer side of the area partitioned into 20 grids.

A flat-top surface area is computed by adding the area of grids which density is 0.95 or larger, This density mesh figure is shown Fig. 8(b). The flat-top surface area is com-

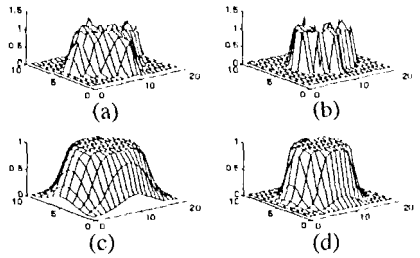

Figure 8: Simulation results of clearance.

puted **to** bc equal to **0.0873.** This value is an approximalion of the real minimum clearance of dian]ond-shape clearance volume, which is 0.0692. Using this area and covariance matrix, Σ, of the simulated samples, an initial T parameter value is calculated, T= 0.6320. However, after the optimization process, we. obtained T= 0.5855. The corresponding analytical Gaussian-Sigmoid distribution, without optimization on Σ, is shown in Fig. 8(c). Finally, optimization is performed on Σ, and the corresponding Gaussian-Sigmoid distribution is shown in Fig. 8(d). From these optimized T and Σ, the axis lengths of [0.1 171, 0.2374] anti [0.2254, 0.4773] (where [x, 0]) are. calculated for the minimum and maximum ellipsoids, respectively. The nominal ellipsoid is calculated to have the axis lengths of [0.1 762, 0.3 S73], with the range of [0.0592, 0.1199].

5: Propagations

Tolerance propagation refers to the effect of tolerance of a mating feature on other mating features in the assembly. Similarly, clearance propagation refers to the effect of clearance between two mating features on other features. In this section, we describe approaches to computing the propagations of tolerances and clearances.

5.1: Serial chain

A serial chain (S-chain) is a path without repeated nodes in a graph (feature graph.) In S-chain, tolerances and clearances propagate from a node to the next node in the chain; and they can bc calculated independently. The propagation of tolerances in S-chain consists of adding the tolerances of a node and its next node. Note that the rotation components of tolerance of a node may create translation components on the next node. This effect must be added.

The operation to acid two tolerance ellipsoids is called a sweep operation, or a Minkowski addition [18]. A sweep operation is defined as an addition of all possible combinations of position vectors of two tolerance samples. The resulting distribution is approximated by Gaussian distribution using the covariance matrix (3) obtained from the added distribution. "1'hen, Chi-Square error reduction scheme is used to optimized the Gaussian distribution.

Now, the method of sweep operation for clearance ellipsoids is to generate a clearance distribution, e.g, flat-top bell shaped. Fig. 9. illustrates this method. First, a boundary B is generated from the swept area of two maximum clearance ellipsoids, as shown in Fig. 9(a). "1'hen, uniform samples are generated inside B, as shown in Fig. 9(b). A randomly generated ellipsoid, from the first clearance ellipsoid and tbc range, is placed at the origin, and a randomly generated ellipsoid, from the second clearance ellipsoid and the range, is placed on every sample, as shown in Fig. 9(c), Finally, those samples which make those two random ellipsoids to intersect are collected, as shown by dark dots in Fig. 9(d). This process is repeated many times, then the distribution of the collected samples is approximated by Gaussian-Sigmoid filter method described in section 3.3.

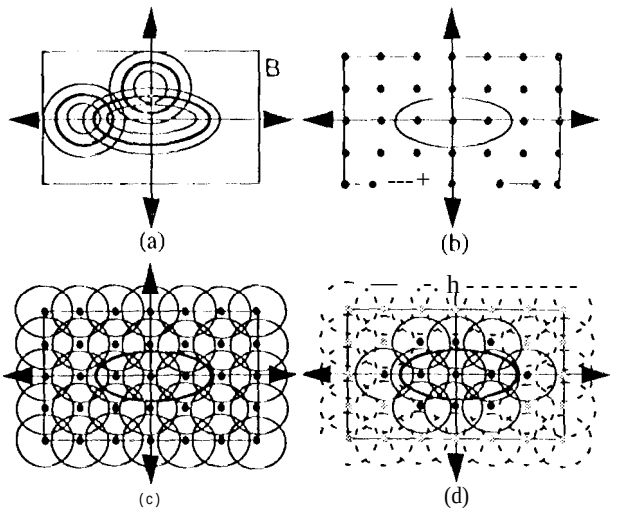

Figure 9: Clearance sweep operation.

Example 1:

The tolerance and clearance at upper hole of P_4 arc computed for a subassembly consisting of parts, P1, P3, and P4 of Fig. 1. in this simulation, clearance was computed twice for two different diameters and dimension tolerances of peg and hole: 1.4010,05 and 1.80± 0.05, and 1.63±0.001 and 1.67± 0.001. Note that all mating features have the same position tolerances as shown in Fig. 4(a). The simulation results are reported. The tolerance ellipsoid is

$$([0.123,\ 0.028], \begin{bmatrix} 0.95 & -0.30 \\ 0.30 & 0.95 \end{bmatrix}),$$

for (axis lengths, rotation matrix). The clearance ellipsoids are

$$([1.523,\ 1.124], \begin{bmatrix} 0.99 & 0.01 \\ -0.01 & 0.99 \end{bmatrix}, [0.300,\ 0.221]) \text{ and}$$

$$([0.1\ S4,\ 0.092], \begin{bmatrix} 0.94 & -0.33 \\ 0.33 & 0.94 \end{bmatrix}, [0.066,\ 0.039]),$$

for (axis lengths, rotation matrix, ranges) for large and small clearances respectively. The results show that the first simulation has much larger clearance than tolerance, as it should bc, since clearances were much larger than tolerances. However, the second simulation has nominal clearance that is closer to tolerance. No[c. that the tolerances come from every mating feature in the chain, whereas the clearances come from every pair of mating features.

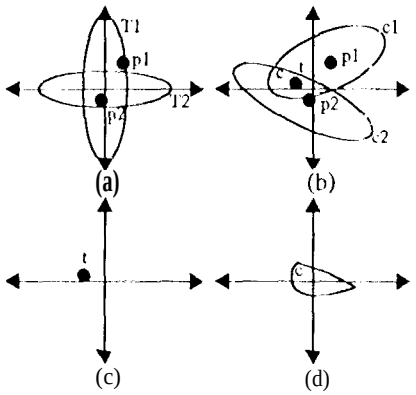

Figure 10: Intersection operation.

5.2: Parallel chain

A parallel chain (P-chain) is a minima] loop, i.e. no subset of its nodes can form a loop, in a feature gi aph. To compute the propagation of tolerances and clearances of a P-chain, we hypothetically cut the P-chain at M-node, and form two S-chains, SC1 and S('2. Here, the clearance of M-node must be added to the S-chain which has the selected 1~-node for the propagation. From the results of SC1 and SC2, a solution for P-chain can be calculated using the intersection operation, which will be explained next.

The method is described using Fig. 10. I .et's assume t t nat T1 and T2 arc the tolerances of SC 1 and SC2, respectively, as shown in Fig. IO(a). With normal distribution, randomly generate one sample from T1 and one from T2, where the centers of T1 and T2 arc located at the origin of a coordinate frame. These samples, p1 and p2, denote instances of tolerance accumulation of SC1 and SC2, respectively. Next, randomly generate clearances, C 1 and C2, from clearances and ranges of SC1 and SC2. C1 and C2 denote instances of clearance accumulation of SC 1 and SC2, respectively. I .ocate centers of C 1 and C2 on p] and p?, respectively, as shown in Fig. IO(b). I'hen, the intersection of C1 and C2 is computed. This intersection area and the center point, c and t respectively, arc the clearance and the toler ance of one instant.c of a I'-cbain. By repeating the above process many times, a distribution of ?'s, as well as C'S, can bc formed. These distributions arc approx - imated using methods described in sections 3.2 and 3.3. Note that the location of t remain the same, but the center of c must be located al the origin of a coordinate. frame as shown in Figs. IO(C) and (d).

The assemblability of a P-chain can be computed by dividing the. number of successful trials by the total number of trials. An assembly is assumed successful if C1 and C2 intersect, or c is not empty.

Example 2:

A subassembly, composed of PI, 1'2, and P3, forms a P-chain. Two S-chains, SC1 and SC2, arc formed by hypothetically cutting the P-chain between P2 and P3.

Two simulation results are shown using two different

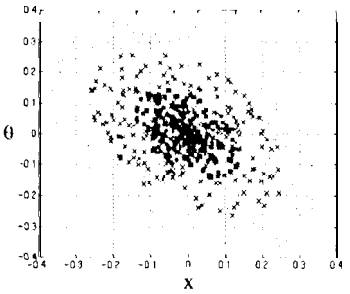

Figure 11: Tolerance and clearance of P-chain.

diameters for pegs and holes as in example 1. With larger clearances, the tolerance ellipsoid is

([0,078, 0.121], [0.74 -0.66 / 66 -0.14]),

and the clearance ellipsoid is

([0.203, 0.320], [0.070 / -0.70 0.71], [0.095,o.150]).

This result is plotted in Fig. 11, where '.', 'x', and '*' arc plots of maximum, nominal, and minimum clearances, respectively, and '-t' is a plot for the. tolerance. 't'he assemblability is equal to 1. With smaller clearances, the tolerance ellipsoid is

([0.014, 0.023], [0.87 0.57 / -0.57 0.82]),

and the clearance ellipsoid is

([0.013, 0.024], [0.73 0.67 / -0.67 0.73] [0,007, 0.0]2]),

The assemblability is equal to 0.946.

S.3: Multi chain

A multi chain (M-chain) is composed of two or more P-chains. To compute the propagation of a M-chain, wc propose a systematic approach. That is, give.n a base node, B-node, and a goal node, (i-node, M-chain can be solved recursively in terms of S-chains and P-chains.

The method is illustrated using Fig. 12. The M-chain consists of two P-chains, ChP1 and ChP2, as shown in Fig. I?(a). First, }'4 is selected as a ~T-node. "1'her), ChP1 is cut at I'3, which is attached to G-node, to form two S-chains, ChS 1 and ChS2, as shown in Fig. 12(b). ChP1 cannot he solved until ChP2 is solved. That is, tolerances and clearances at P2 and P3 must be computed from ChP2. Since ChP2 is just a P-chain, the solutions can bc computed easily. Note. that, a M-chain may still be a M-chain with one less P-chain after cutting one P-chain, the above step can be recursively applied to a ncw M-chain. The result of ChP2 is propagated to P_3^1 though ChS1 from 1'3. Similarly, the solution propagates to P_3^2 from P2. Lastly, the intersection operation is applied to the results of ChS 1 and ChS2.

The time complexity of M-chain algor ithm in the worst case is $0(2^{n})$, where n is the is the number of P-chains in a M-chain. In the worst case, M-chain is a complete graph and n is $O(m^3)$, where m is the number of parts

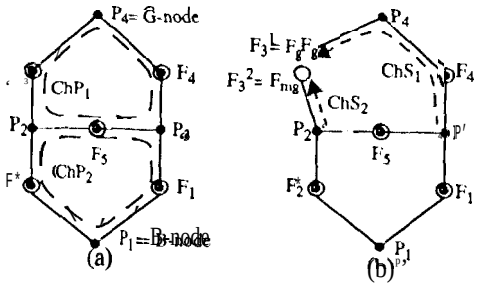

Figure 12: M-chain propagation,

in a M-chain, It requires at least three nodes to form a P-chain. There are $\binom{m}{3}$ feasible P-chains. The recursive process of M-chain algorithm solves two M-chains with onc P-chain less than the previous step. On the way back from the recursion, it solves the P-chain. Therefore, there arc $O(2^n)$ P-chains to be solved.

6: Assemblability

The assemblability of an assembly can be measured from the. product of assemblabilities of all P-chains in a M-chain. If there are n P-chains in a M-chain, assemblability measures of n P-chains are multiplied.

The probability of successfully adjusting a part feature to its nominal pose can be measured statistically using Monte-Carlo simulation. For example, N samples are randomly and normally generated from the tolerance ellipsoid of a M-chain. Then, M clearance ellipsoids are generated randomly. Now, count the tolerance samples, Ni, that intersect with a clearance ellipsoid for M clearance ellipsoids. Using the equation,

$$\left(\sum_{i=1}^{M} N_i \right) / (M \times N)$$

this measure can be calculated.

7: Conclusion

Tolerance affects not only the functionality and manufacturability but also the assemblability of a product. For the assemblability analysis, we have proposed a statistical representation of tolerance and clearance. Tolerance is represented by an ellipsoid, and clearance is represented by an ellipsoid and a range, Gaussian distribution is assured for tolerances. Moreover, Monte-Carlo method is used with Gaussian distribution, Gaussian-Sigmoid distribution, and Chi-Square error reduction scheme to approximate the tolerance and clearance. Algorithms are. proposed for serial, parallel, and M-chains for the propagation of tolerances and clearances. We have shown that clearances play an important role in the assemblability evaluation, because they can be used to compensate for tolerance, although clearances may cause instability of a product if clearances arc large.

References

[1] O. Bjorke, Computer-Aided Tolerancing, ASME Press, New York, 1989.

[2] L. W. Foster, GEO-METRIC II I: The Application of Geometric Dimensioning and Tolerancing techniques (Using the Customary Inch System), Addison-Wesley Pub., 1994.

[3] Dimensioning and Tolerancing, ANS1 Y 14.5M, American Society of Mechanical Engineering, USA, 1982,

[4] D. E. Whitney and O. 1. Gilbert. "Representation of Gee. metric Variations Using Matrix Transformations for Statistical Tolerance Analysis in Assemblies," *Proc. of IEEE International Conference on Robotics rind Automation*, pp. 314321, 1993,

[5] A. A. G. Requicha, "Toward a Theory of Geometric Tolerancing," *The International Journal of Robotics Research*, 2(4), pp. *40-60, 1983.*

[6] A. A.-G. Requicha, "Representation of Tolerances in Solid Modeling: Issues and Alternative Approaches," *Solid Modeling by Computers: From Theory to Applications,* J. W. Boyse and M. S. Pickett, Eds. New York: Plenum, pp. 3-22, 1984.

[7] P. Treacy and et al., "Automated Tolerance Analysis for Mechanical Assemblies Modeled wirh Geometric Features and Relational Data Structure," *Computer-Aided Design, vol. 23,* no. 6, pp. 444-453, 1991.

[8] N. Wang and T. M. Ozsoy, "Automatic Generation of Tolerance Chains from Mating Relations Represented in Assembly Models," *Journal of Mechanical Design, vol.* 115, pp. 757-761, 1993,

[9] R. Soderberg, "CATI: A computer Aided Tolerancing Inter face," DE- *Vol.* 44-2, *ASME Advances in Design Automation, vol.* 2, pp. 157-164, 1993.

[10] S. F. Su and C. S. G. Lee, "Uncertainty manipulation and Propagation and Verification of Applicability of Actions in Assembly Tasks," *Proc. of IEEE International Conference on Robotics and Automation*, pp. 2471-2476, 1991.

[11] D. Shalon, D. Gossard, K. Ulrich, and D. Fitzpatrick, "Representing Geometric Variations in Complex Structural Assemblies on CAD Systems," *DE-Vol.44-2, Advances in Design Automation, ASME*, vol. *2*, pp. 121-*132*, 1992.

[12] D. Grossman, "Monte Carlo Simulation of Tolerancing in Discrete Parts manufacturing and Assembly," *Stanford Artificial intelligence Laboratory Memo AIM-280, Computer Science Department Report No. STAN-CS-76-555*, May 1976.

[13] H. Ko and K. Lee, "Automatic Assembling Procedure Generation from Mating, Conditions," *Computer-Aided Design, vol. 19,* no. 1, pp. 3-10, 1987.

[14] J. Stark and J. W. Woods, Probability, Random Processes, and Estimation Theory for Engineers, Prentice Hall, 1986.

[15] 1. M. Sobol, A Primer for the Monte Carlo Method, CRC Press Inc., 1994.

[16] A. E. Bryson and Y-C. Ho, Applied Optimal Control, John Wiley and Sons, New York, 1975.

[17] G. Strang, Linear Algebra and Its Applications, Harcourt Brace Jovanovich, 1986.

[18] P. Ghosh, "A Mathematical Model for Shape Description Using Minkowski Operators," *Computer Vision, Graphics, and Image Processing,* vol. 44, no. 3, pp. 239-269, 1988.

Acknowledgement

The research described in this paper was in part carried out by the Jet Propulsion la,horatory, California Institute of Technology, under a contract with the National Aeronautics and Space Administration.